Hysteresis and self-organized criticality in the O(N) model in the limit N to infinity

1992 J. Phys. A: Math. Gen. 25 4967

(http://iopscience.iop.org/0305-4470/25/19/012)

J. Phys. A: Math. Gen. 25 (1992) 4967–4984. Printed in the UK

Hysteresis and self-organized criticality in the O(N) model in the limit $N \to \infty$

Deepak Dhar† and Peter B Thomas‡

Theoretical Physics Group, Tata Institute of Fundamental Research, Homi Bhabha Road, Bombay 400 005, India

Received 19 February 1992

Abstract. We consider the response of the ferromagnetic N-vector model to a sinusoidally varying external magnetic field in the large-N limit. In all dimensions $d > 2$, we show that at low frequencies ω, and small amplitudes H_0 of the field, the area of the hysteresis loop scales as $(H_0\omega)^{1/2}$ with logarithmic corrections. At very high frequencies, the area varies as H_0^2/ω. We find that for any H_0 there is a dynamical phase transition separating these two frequency regimes. We determine numerically the critical frequency as a function of the field strength. In the high-frequency phase the magnetization is predominantly transverse to the external magnetic field.

1. Introduction

The basic phenomenology of hysteresis has been known for a long time. In the simplest setting, hysteresis can be observed when a system is driven away from equilibrium by a periodic perturbation. It is particularly noticeable near a first-order phase transition. The familiar S-shaped hysteresis loops are widely used as the signal of first-order phase transitions, in the laboratory and in Monte Carlo simulations. However, at present there is no satisfactory statistical mechanical theory of hysteresis starting from the microscopic dynamics. In this paper, we study the hysteretic response of an isotropic ferromagnetic system, to an external, oscillating magnetic field. A better understanding of hysteresis may also have technological applications, for example in designing the materials of transformer cores.

There are qualitatively two kinds of magnetic systems, namely Ising-like systems and continuous-spin systems. In Ising-like systems, the system has to cross a free-energy barrier for the order parameter to change sign (in a d-dimensional system of size L the barrier height goes as JL^{d-1} where J is the exchange coupling), while in isotropic continuous-spin systems, the magnetization vector can turn without encountering any free-energy barrier. Hysteresis in systems with a free-energy barrier has been studied by many authors [1–8]. Agarwal and Shenoy [1] studied hysteresis in a one-component order parameter system, in which the free energy has two competing minima separated by an energy barrier. Fluctuations which enable the order parameter to cross the energy barrier were modelled by Gaussian white noise. This work was

† Email address: ddhar@tifrvax.bitnet.

‡ Email address: peter@tifrvax.bitnet.

0305-4470/92/194967+18$04.50

extended by Mahato and Shenoy [2], to find the first passage time probability distribution in this model. While such a description explains the gross phenomenological features of hysteresis in many systems, it is essentially a mean-field approximation, ignoring the effects of short-range correlations. Tomé and de Oliveira [3] have studied the response of the two-dimensional Ising model to a time-dependent oscillating magnetic field in the mean-field approximation. They ignored the microscopic fluctuations and obtained a single differential equation for the magnetization, describing a particle in an oscillating double-well potential without noise. Jung *et al* [4] have also studied the hysteretic response of bistable systems in a similar model. None of the above descriptions include the effects of spatial fluctuations in the order parameter.

There has been relatively less work on hysteresis in spatially extended, interacting systems. In two recent important papers Rao *et al* [5] (RKP) have studied hysteresis in interacting spin systems. In them, they also studied hysteresis in the two-dimensional Ising model by Monte Carlo simulations. Acharyya and Chakrabarti [6] have made similar simulations in two to four dimensions. Lo and Pelcovits [7] extended the work of RKP to larger systems. They found evidence for a dynamical phase transition in the problem, and estimated scaling exponents for the area of the hysteresis loops. A numerical simulation of the hysteretic response of a 2D scalar ϕ^4 field in the presence of an external sinusoidal field using cell-dynamics, was made by Sengupta *et al* [8]. Their results were in good qualitative agreement with Lo and Pelcovits.

Amongst these papers, only RKP deal with hysteresis in continuous, interacting spin systems. They studied hysteresis in the three-dimensional $O(N \to \infty)$ model in the presence of sinusoidal and pulsed external fields by numerical integration of the equations of motion. They found numerical evidence for the existence of a dynamical phase transition at sufficiently high frequencies. That is, they found that for any field strength H_0, there appears to exist a corresponding critical frequency $\omega_c(H_0)$, so that for $\omega > \omega_c(H_0)$ the loops do not possess inversion symmetry. RKP also studied the H_0 and ω dependence of the area of the hysteresis loops. An important observation they made was that at low frequencies the area of the hysteresis loops has a power-law dependence on the amplitude and the frequency of the external field, i.e. the area scales as $H_0^{\alpha}\,\omega^{\beta}$. Their numerical estimate of these exponents were $\alpha \simeq \frac{2}{3}$ and $\beta \simeq \frac{1}{3}$.

In this paper, we study the response of a continuous spin system to a sinusoidal external field. We consider the ferromagnetic N-vector model with dissipative dynamics in the limit $N \to \infty$. This is the same model as studied by RKP. Like them, we study the shape dependence of the hysteresis loops as a function of the amplitude and frequency of the external field. However, our detailed results differ from theirs in some important ways. Firstly, we find that the stable hysteresis loops retain their inversion symmetry for all field amplitudes and frequencies. However as the frequency of the external field is increased, there *is* a dynamic phase transition to a phase where the magnetization is predominantly transverse to the direction of the magnetic field. We obtain the critical curve numerically. For small H_0 and ω, we show that the area of the hysteresis loop scales as $(H_0\omega)^{1/2}$ with logarithmic corrections. The slowly-varying corrections to scaling are presumably responsible for the difference between the asymptotic exponents $\alpha = \beta = \frac{1}{2}$ and the effective exponents determined numerically by RKP.

The paper is organized as follows. The model is defined in section 2, and the integro-differential equations resulting from the dynamics are derived. In section 3 we rewrite the dynamical equations taking into account the possibility of a non-zero

transverse magnetization in the system. Section 4 summarizes our numerical work. We show the typical behaviour of various dynamical variables for different amplitudes and frequencies of the external magnetic field. We also solve for the critical curve in the space of the amplitude and the frequency of the field. In section 5 we study theoretically the qualitative behaviour of the differential equations at low frequencies to estimate the area of the hysteresis loop in the limit of small fields and frequencies, and hence determine the scaling exponents α and β. We also obtain the high-frequency behaviour of the system, including the asymptotic form of $\omega_c(H_0)$ for small and large H_0 analytically. In section 6, we summarize our results and argue that the scaling exponents at low and high frequencies obtained in this model are generally true for all continuous-spin systems. We also point out that the occurence of such robust power laws in this problem may be viewed as a particular example of self-organized criticality.

2. The N-vector model

We consider an N-dimensional vector field ϕ in a d-dimensional space whose Hamiltonian is given by

$$\mathcal{H} = \frac{1}{V}\int \mathrm{d}^d x \left(\frac{1}{2}(\Delta\phi)^2 - \frac{r}{2}\phi\cdot\phi + \frac{u}{4N}(\phi\cdot\phi)^2 - \boldsymbol{H}\cdot\phi\right). \tag{1}$$

We study the time evolution of this model. This is assumed to be governed by dissipative Langevin dynamics, the equations of motion being

$$\frac{\partial\phi(\boldsymbol{x})}{\partial t} = -\frac{1}{2}\frac{\delta\mathcal{H}}{\delta\phi(\boldsymbol{x})} + \beta(\boldsymbol{x},t). \tag{2}$$

The unit of time is chosen so that the coefficient of $\delta\mathcal{H}/\delta\phi$ is $-\frac{1}{2}$. $\beta(\boldsymbol{x},t)$ is Gaussian white noise satisfying

$$\langle\beta(\boldsymbol{x},t)\rangle = 0 \qquad \langle\eta_i(\boldsymbol{x},t)\eta_j(\boldsymbol{x}',t')\rangle = T\,\delta_{ij}\,\delta(\boldsymbol{x}-\boldsymbol{x}')\,\delta(t-t'). \tag{3}$$

These equations are known to give the correct equilibrium behaviour if the magnetic field H is independent of time. It is reasonable to assume that the microscopic dynamics is unchanged if H depends on time. The relaxation to equilibrium in this model was first discussed by Mazenko and Zannetti [9]. Let the first component of ϕ be in the direction of the magnetic field H. Since all the transverse modes are equivalent, assuming *no symmetry breaking*, $\langle\phi_i\rangle$ vanishes except when $i = 1$. Define $m(t)$ and $\delta\phi_i(\boldsymbol{x},t)$ by

$$\langle\phi_i(\boldsymbol{x},t)\rangle = m(t)\,\delta_{i,1} \qquad \delta\phi_i(\boldsymbol{x},t) = \phi_i(\boldsymbol{x},t) - \langle\phi_i(\boldsymbol{x},t)\rangle. \tag{4}$$

The angular brackets denote the stochastic average over the noise. Let

$$C_i(\boldsymbol{x}-\boldsymbol{x}',t) = \langle\delta\phi_i(\boldsymbol{x},t)\delta\phi_i(\boldsymbol{x}',t)\rangle \tag{5}$$

and its Fourier transform be $C_i(\boldsymbol{q},t)$. In the limit of $N\to\infty$, many simplifications occur. In this limit, it has been shown [9] that $m(t)$ and $C_i(\boldsymbol{q},t)$ $(i\neq 0)$ get decoupled from the longitudinal mode $C_1(\boldsymbol{q},t)$. Using the symmetry of the transverse

modes, the subscript i can be dropped, and any of the perpendicular modes are described by $C_\perp(q,t) \equiv C_q(t)$. The equations for the $C_q(t)$s close on themselves and do not involve higher-order correlation functions [9]. One then finds that the rescaled $m(t)$ and $C_q(t)$ evolve according to

$$\frac{\mathrm{d}m}{\mathrm{d}t} = \frac{1}{2}\left[A(t)m(t) + H(t)\right] \qquad \frac{\mathrm{d}C_q}{\mathrm{d}t} = T - \left[q^2 - A(t)\right] C_q(t) \tag{6}$$

where

$$A(t) = r - um(t)^2 - uS(t) \tag{7}$$

and $S(t)$ is the total fluctuation per transverse component of ϕ at time t

$$S(t) = \frac{1}{(2\pi)^d} \int \mathrm{d}^d q\, C_q(t)\,. \tag{8}$$

C_q has spherical symmetry. An ultra-violet cut-off at $q_{\max}$ has to be introduced to make the problem well defined. This is chosen, by analogy with the natural Brillioun zone cut-off in lattice models, to be such that the volume of a sphere in the d-dimensional momentum space is $(2\pi)^d$. This gives

$$q_{\max} = 2\sqrt{\pi}\left(\frac{d}{2}\,\Gamma(d/2)\right)^{1/d}. \tag{9}$$

We choose the time dependence of the external magnetic field to be a simple sinusoidal function $H(t) = H_0 \sin \omega t$. These equations are essentially the same as those studied earlier by RKP.

These equations can be easily solved in the special case when the magnetic field H is independent of time (the $\omega \to 0$ limit). In this case the system relaxes to its thermodynamical equilibrium state after large times. The steady-state (equilibrium) value of the magnetization $m_{\mathrm{eq}}(H)$ is obtained by equating the various derivatives in (6) to zero, giving

$$\begin{aligned} 0 &= rm_{\mathrm{eq}}(H) - um_{\mathrm{eq}}^3(H) - um_{\mathrm{eq}}(H)S(H) + H \\ C_q(H) &= \frac{T}{q^2 + H/m_{\mathrm{eq}}(H)}\,. \end{aligned} \tag{10}$$

We can solve for $m_{\mathrm{eq}}(H)$ from these equations and (8).

The behaviour of $m_{\mathrm{eq}}(H)$ is well known from the equilibrium statistical mechanics of the N-vector model. In one or two dimensions there is no ferromagnetic phase transition and hence no jump discontinuity in m at zero field, when T is finite. In three or more dimensions, there is a jump discontuity in m at $H = 0$, below a critical temperature T_c. In three dimensions, $\mathrm{d}m/\mathrm{d}H$ has a square root singularity at $H = 0$ below T_c, while in four or more dimensions its value is finite. The spontaneous magnetization in d dimensions ($d > 2$) when $T < T_c$ is

$$m_0 = \pm\sqrt{\frac{r}{u} - \frac{T\,d}{(d-2)\,q_{\max}^2}}\,. \tag{11}$$

T_c is the temperature above which $m_0 = 0$.

When the frequency is non-zero the situation is more complicated, and non-equilibrium effects come into play. We shall only consider the case when $d > 2$, when there is spontaneous magnetization. At small but finite frequencies the graph of m versus H is the familiar hysteresis loop (see figure 1 later). When the frequency is sufficiently small so that the timescales associated with the relaxation of the system become much smaller than $1/\omega$, the hysteresis loop should approach the equilibrium curve, and hence its area should shrink to zero. If the frequency or the amplitude of the external field is increased, the area of the loop initially increases. It reaches a maximum, and for larger frequencies it decreases again. From a numerical solution of (6), (7) and (8) RKP saw that at low frequencies and fields, the area W of the loops could be fitted to a power law,

$$W \sim H_0^{\alpha} \omega^{\beta} \tag{12}$$

with $\alpha \simeq \frac{2}{3}$ and $\beta \simeq \frac{1}{3}$. In the following we show that the power-law behaviour is correct, but with $\alpha = \beta = \frac{1}{2}$.

3. The existence of transverse magnetization

The question of whether there exists a dynamical phase transition in the model is an important one. In the limit of high frequencies, the spin system cannot respond to the external magnetic field. Hence the magnetization vector is expected to oscillate around any initial direction with magnitude $m \simeq m_0$. Thus at high frequencies, there may be a dynamical phase transition, with a new phase where the hysteresis loops do not possess inversion symmetry. This has been observed numerically by RKP. A difficulty with their treatment is that they have ignored the possibility of a non-zero transverse magnetization in the steady-state solution, since the direction in which the spins align need not be parallel to the external field. In terms of (6), C_q can have a delta function at $q = 0$. For numerical accuracy it is important to take this into account explicitly. Therefore we write

$$C_q(t) = (2\pi)^d m_\perp^2(t)\delta(q) + \tilde{C}_q(t). \tag{13}$$

With this, we can rewrite the equations of motion (6), (7) and (8) as

$$\begin{aligned} &\frac{\mathrm{d}m}{\mathrm{d}t} = \frac{1}{2}[A(t)m(t) + H(t)] \qquad \frac{\mathrm{d}m_\perp^2}{\mathrm{d}t} = A(t)m_\perp^2(t) \\ &\frac{\mathrm{d}\tilde{C}_q}{\mathrm{d}t} = T - [q^2 - A(t)]\,\tilde{C}_q(t) \end{aligned} \tag{14}$$

where

$$\begin{aligned} A(t) &= r - um(t)^2 - um_\perp^2(t) - u\tilde{S}(t) \\ \tilde{S}(t) &= \frac{1}{(2\pi)^d}\int_{|q|\leqslant q_{\max}} \mathrm{d}^d q\, \tilde{C}_q(t). \end{aligned} \tag{15}$$

It is clear that (14) permits a solution with $m_\perp^2 = 0$ at all times, which is the solution obtained by RKP. This is also the thermodynamically stable solution in the

presence of a constant field H. However, if the field $H = 0$, then non-zero values of $m_\perp^2$ are allowed satisfying $m^2 + m_\perp^2 = m_0^2$, by the O(N) symmetry of the problem. In general, the solution with $m_\perp^2 = 0$ need not be stable for all H_0 and ω. In order to check the stability of the solution with $m_\perp^2 = 0$, we can formally integrate (14) to get

$$m_\perp^2(t + 2\pi/\omega) = m_\perp^2(t) \exp\left[\oint A(t')\,dt'\right] \tag{16}$$

where $\oint$ implies integration over a period $2\pi/\omega$. From this it follows that the $m_\perp^2 = 0$ solution is unstable if

$$\oint A(t')\,dt' > 0\,. \tag{17}$$

When the system is in thermal equilibrium in the presence of a constant field H, the solution with $m_\perp^2 = 0$ is stable, because

$$A(H) = -\frac{H}{m_{eq}(H)} \tag{18}$$

which is always negative.

By continuity, the solution with $m_\perp^2 = 0$ is also stable at low frequencies. However at high frequencies, the average value of $A(t)$ over a cycle becomes positive if $m_\perp^2$ is held at zero, implying an instability in this solution. If $\oint A(t)\,dt > 0$, the average value of $m_\perp^2$ increases with time. But increasing $m_\perp^2$ will decrease the growth rate A [from (15)]. In the steady state, the amplitude of $m_\perp^2$ reaches a value such that $\oint A\,dt$ becomes equal to 0. Hence the stable steady-state behaviour of (14) and (15) at high frequencies is a solution with $m_\perp^2 \neq 0$. We find that then the average of $m(t)$ over a complete cycle is zero at all frequencies. This implies that at high frequencies, the spins align coherently in a direction *transverse* to the applied magnetic field, and $m(t)$ *never* loses its inversion symmetry. There is a curve in the H_0–ω plane separating regions between which $m_\perp^2 = 0$ and $m_\perp^2 \neq 0$. This phase transition is qualitatively different to the dynamical phase transition in hysteresis that has been discussed so far [3–5, 7, 8], where at high frequencies $\oint m(t)\,dt \neq 0$.

The onset of transverse magnetization by an oscillating magnetic field may seem counter-intuitive at first. This can be understood in the following way. The exchange energy (the dominant energy in the problem) is minimized if the magnitude of the total magnetization vector is non-zero at all times. Only its *direction* can vary significantly in time. Consider the total magnetization vector of the system. At low frequencies it is possible for the magnetization to follow the direction of the external field, and the fractional amount of time spent in magnetization reversal (the only time when the transverse components are significant) is small. As the time period is decreased, this fraction increases. If the field is oscillating too fast, the average spin direction cannot follow the field. At this level of approximation all directions are equivalent, and at high frequencies the magnetization vector can make small oscillations of order $1/\omega$ about any arbitrary initial direction. However, a spin transverse to the field can respond more readily to a changing field than one that is parallel to the field (the restoring force is proportional to the sine of the angle between the field and the magnetization vector). In addition, since the phase space for an N-dimensional

spin is much larger in the transverse directions, it follows that at high frequencies an overall transverse direction of magnetization would be favoured, compared with a longitudinal direction. By this argument, we would also expect a similar phase transition to occur at large frequencies in the N-vector spin model for finite N.

4. Numerical results

We have to integrate (14) and (15). These are nonlinear, and the only known way of solving them is by numerical integration. The dynamical variables $m(t)$ and $m_\perp^2(t)$ depend on $A(t)$, which is a function of m, $m_\perp^2$ and $\tilde{S}$, the integral of $\tilde{C}_q$ over all the momenta. It is useful to define the new variables $F(q)$

$$F(q) \equiv \left(\frac{d}{q_{\max}^d}\right) \tilde{C}_q \, q^{d-1}$$

so that

$$\tilde{S}(t) \equiv \int_0^{q_{\max}} F(x)\,\mathrm{d}x\,.$$

From (6), $F(q)$ satisfies the equation

$$\frac{\mathrm{d}F(q)}{\mathrm{d}t} = \left(\frac{d}{q_{\max}^d}\right) T\, q^{d-1} - \left[q^2 - A(t)\right] F(q)\,.$$

In order to evaluate $\tilde{S}(t)$, we choose special values of q, and estimate the integral by Gaussian quadrature. These equations along with the equations for $m(t)$ and $m_\perp^2(t)$ in (14) and (15) form a system of nonlinear, coupled differential equations.

In our numerical analysis, we have worked in $d = 3$ dimensions. To find the relevent parameter range, we note that typically the critical temperature of ferromagnets is of the order of hundreds of degrees Kelvin, while the maximum fields are less than a few thousands of Gauss. The reduced magnetic field is therefore less than one degree Kelvin, so in our units the region of interest is when $H_0 \ll T_c$. The frequency associated with spin relaxation is of the order of 10^8 Hz (which is unity in our units). For fields of the order of a few Gauss, the ferromagnetic resonance frequency in ferrites is of the order of 10^9 Hz ($\omega \approx 10$ in these units). Hence in the laboratory, it is possible to study hysteretic behaviour in ferrites, on both the low-frequency side of the ferromagnetic resonance frequency when $\omega \ll H_0$ and also the high-frequency side, when $\omega \gg H_0$. We have chosen $r = u = 0.1$. With this choice, $T_c = (6\pi^2)^{2/3}/3 \approx 5.0642$. The temperature was chosen to be $T = 1$, which is well below T_c.

For very small values of H_0, when r, u and $q_{\max}$ are much larger than H_0, these equations become 'stiff', and standard integration packages like the Runge–Kutta method take a long computation time. Of the several integration techniques we tried, we found that the Richardson extrapolation method [10] worked best. In this technique, the key idea is to use a set of difference equations with various step sizes Δt to evaluate a sequence of approximations to the dynamical variables after a macroscopic time step, and estimate their values in the limit $\Delta t \to 0$ by rational

function extrapolation. We have chosen the sub-intervals Δt to be sufficiently small, so that the extrapolation errors were within 10^{-4}.

Normally the difference equations for time intervals Δt are generated by the 'modified-midpoint method', and the whole procedure is known as the 'Bulirsch–Stoer algorithm' [10]. However these equations are so stiff that no advantage is gained over conventional methods like the Runge–Kutta, unless the difference equations used are stable when Δt is large. Our choice for the difference equations is based on the observation that if $A(t)$ is known, then the equations for m, $m_\perp^2$ and $\tilde{C}_q$ are linear, and decouple from each other (14). The difference equations were generated by keeping A constant and equal to its value at the beginning of each sub-interval, and then using the explicit integrated functions over finite time intervals. It is clear that in the limit $\Delta t \to 0$, the differential equations can be derived from them. This procedure considerably reduced the problem of stiffness at very low frequencies. However, at high frequencies the variable step fourth-order Runge–Kutta method worked more efficiently.

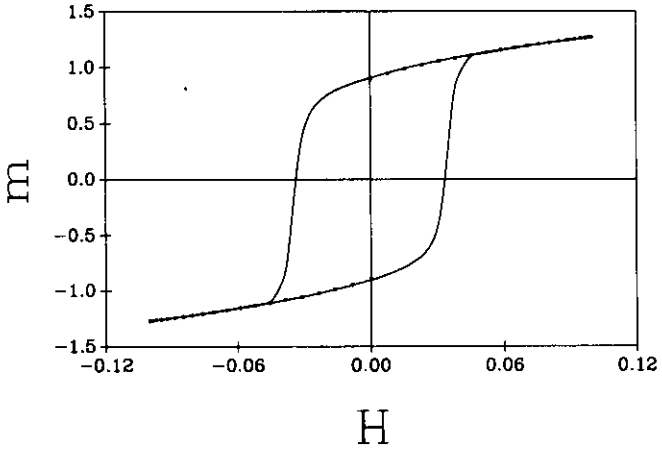

Figure 1. A typical hysteresis loop (the values used for this graph were $H_0 = 0.1$ and $\omega = 0.001$). Superposed on this are the points corresponding to equilibrium.

We find two qualitatively different regimes in the H_0–ω space, separated by the critical curve. In figures 1 to 6, we show the typical behaviour of the dynamical variables in each of these regimes. The response of the system in the low-frequency regime is shown in figures 1–4. Figure 1 shows a hysteresis loop for $H_0 = 0.1 \simeq 0.02\,T_c$ at a frequency $\omega = 0.001$. The m–H equilibrium curve is superposed in this figure. We find that the slope of the hysteresis loop is small and comparable to that of the equilibrium curve, except for the relatively short periods when $m(t)$ changes sign. In figure 2 we show the response of the transverse fluctuations $\tilde{S}$ to the time variations in $H(t)$. The value of $\tilde{S}$ is seen to be quite small when $|m|$ is large. It starts rising as $|m|$ decreases, and rises to a value near r/u soon after $m(t)$ changes sign, and then quickly falls again to small values. This is obvious, as when the magnetization is parallel to the field, the transverse fluctuations are small, but as the spins turn, the transverse fluctuations become significant, of the order of the square of the spontaneous magnetization. For sufficiently small ω, $m_\perp^2$ was found to vanish, implying the absence of transverse long-range order at low frequencies. In figure 3 we plot $\tilde{C}_q(t)$ versus q at various times $t_1 < 0$, $t_2 \sim 0$ and $t_3 = t_c$, where t_c is the coercive time (the time at which m changes sign), to show the behaviour of

the various momentum modes at different times. In figure 4 we have plotted $\tilde{C}_q(t)$ versus ωt when the magnetic field sweeps from negative to positive values, at $q = 0$, $q = q^*$ (defined in (29)) and $q = 3q^*$.

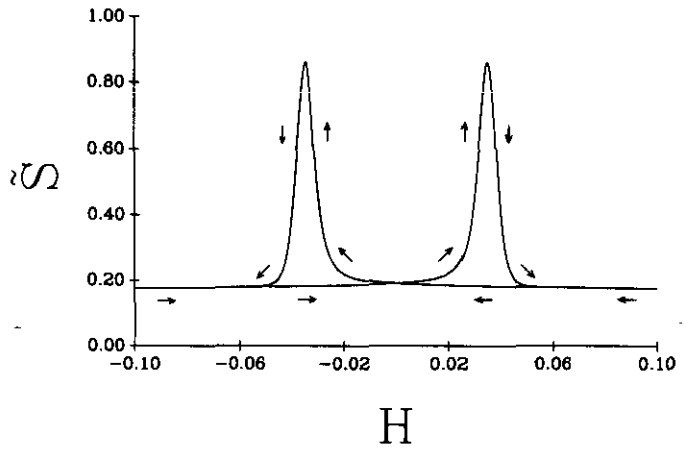

Figure 2. The loop of $\tilde{S}$ versus H, when $H_0 = 0.1$, $\omega = 0.001$.

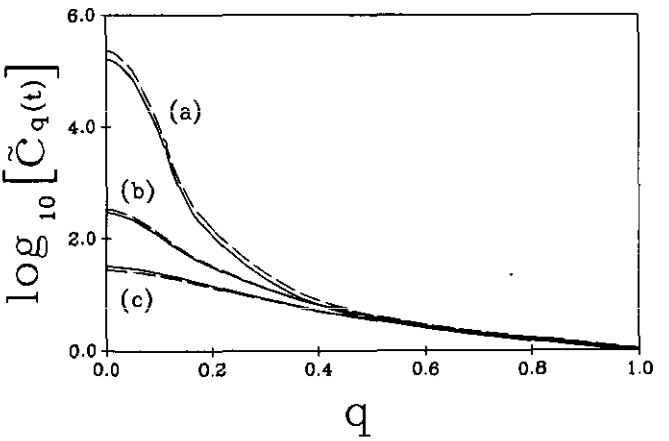

Figure 3. Graph of $\tilde{C}_q(t)$ versus q for $H_0 = 0.1$, $\omega = 0.001$ (a) at $H(t_1) \simeq -0.03$, (b) at $H(t_2) \simeq 0.01$ and (c) at the coercive field $H(t_3) \equiv H(t_c) \simeq 0.032$. The broken curves correspond to the theoretical approximation (26).

Figure 5 shows the hysteresis loop precisely at the phase boundary between the low-frequency phase and the high-frequency phase. The values used are $H_0 = 0.015$ and $\omega \simeq 0.002$. The characteristic loops on the phase boundary are squarish. As in the low-frequency case, the slope of the two branches of the loop is comparable to that of the equilibrium curve except in the short interval when m changes sign (which in this case is near $H = \pm H_0$). Also in figure 5 is superposed a graph of $\tilde{S}$ versus the field H at the same frequency. We note that $\tilde{S}$ is small except when $H(t)$ is near the values $\pm H_0$, the coercive field.

In figure 6 we show a typical high-frequency loop. In this regime, $m_\perp^2$ is non-zero. Superposed are the graphs of $\tilde{S}$ and $m_\perp^2$ versus H. We see that $\tilde{S}$ and $m_\perp^2$ are approximately constant in this graph, and that the m-loop is almost an ellipse.

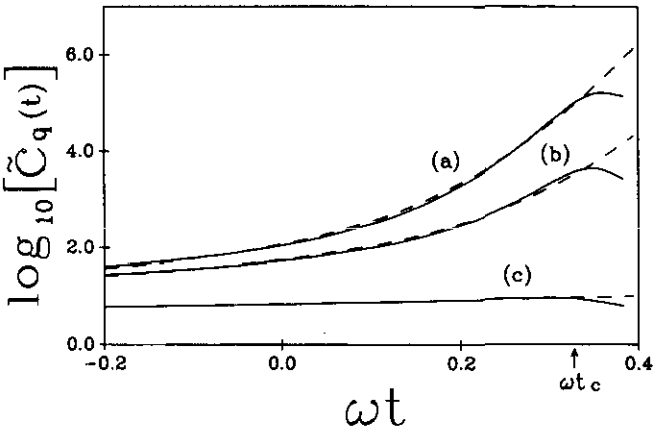

Figure 4. Graph of $\tilde{C}_q(t)$ versus ωt when the field is swept from negative to positive values ($H_0 = 0.1$, $\omega = 0.001$), at $q = 0$, $q = q^*$ and $q = 3q^*$. The broken curves are the approximate solution from (26). The approximation is excellent up to the coercive time t_c, which is indicated in the graph.

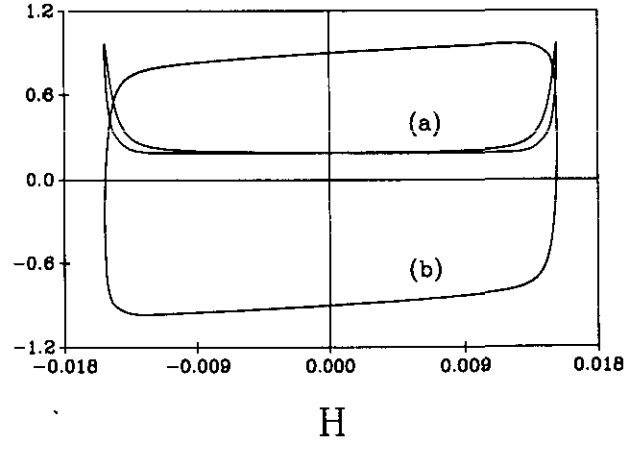

Figure 5. Critical loops at $H_0 \simeq 0.015$ and $\omega \simeq 0.002$. (a) is the loop of $\tilde{S}$ versus H, and (b) is the m–H loop. At higher frequencies, $\tilde{S}$ tends to become constant, and the m–H loop becomes less tilted and elliptical.

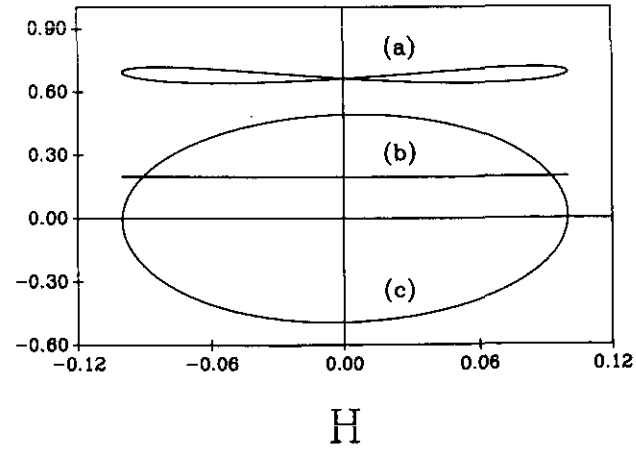

Figure 6. Loops in the high-frequency phase when $H_0 = 0.1$ and $\omega = 0.1$. (a) The loop of $m_\perp^2$ versus H, (b) $\tilde{S}$ versus H, and (c) m versus H. At higher frequencies, $m_\perp^2$ tends to become constant.

This agreement gets better as the frequency is increased, and is explained in the next section.

One can determine the critical curve separating the $m_\perp^2 = 0$ solution from the $m_\perp^2 \neq 0$ solution, by solving for the steady-state behaviour, always keeping $m_\perp^2 = 0$ and finding where $\oint A(t)\,dt$ changes sign. The result is shown in figure 7. At very large frequencies, H_c has an approximately linear dependence on ω. The slope agrees well with the analytic high-frequency limit $H_c = 2\sqrt{2}\,m_0\,\omega$, derived in the next section. At smaller frequencies, we find numerically that the frequency dependence of the critical field is well described by $H_c \simeq b\omega \ln[c/\omega]$ with $b \simeq 1.6$ and $c \simeq 0.25$. A plausibile argument for this functional form is also given in the next section. In figure 8 we show the behaviour of the area of the loop W versus the frequency ω, when $H_0 = 0.1$. There appears to be a derivative discontinuity in this curve as the critical frequency is crossed.

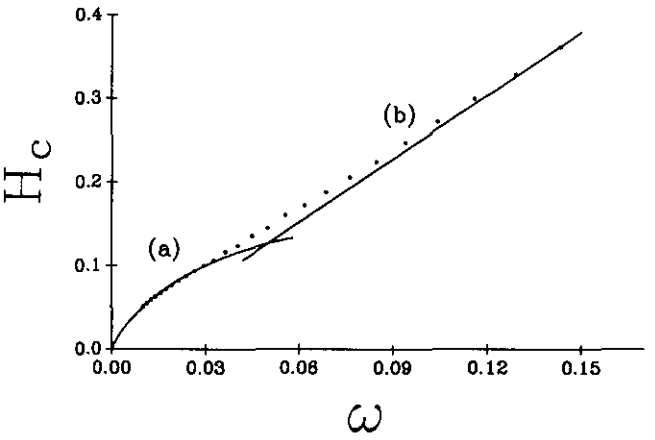

Figure 7. The critical curve in the H_0-ω plane. The points are the numerical data. The full curve (a) is the functional fit $H_c = b\ln(c/\omega)$, with $b = 1.581$ and $c = 0.2488$. The full curve (b) is the asymptotic formula for large ω, $H_c = 2\sqrt{2}\,m_0$. Beyond $\omega \simeq 0.15$, the agreement becomes nearly perfect.

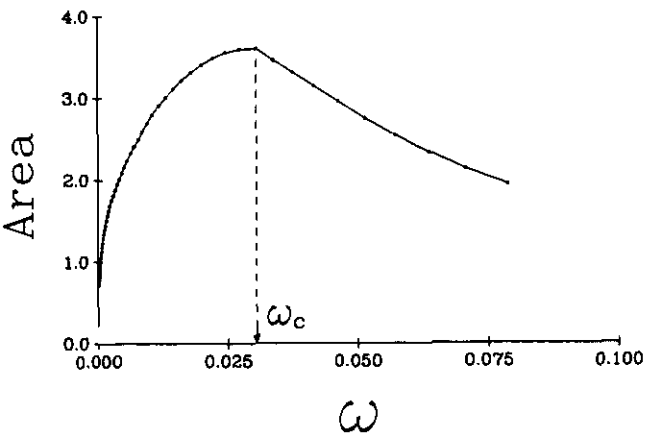

Figure 8. Graph of the area of the hysteresis loop versus ω when $H_0 = 0.1$. $dW/d\omega$ appears to have a discontinuity at $\omega = \omega_c(H_0) \simeq 0.0295$.

5. Theoretical results and scaling exponents

The asymptotic behaviour of the area of the hysteresis loops for ω tending to zero or infinity can be determined theoretically. Consider first the case when $\omega \to 0$.

In this limit, the hysteresis loops look squarish and can be approximated as being made up of four branches (figure 9). As we increase the field slowly from large negative values to small positive values, the magnetization is roughly constant, and increases slowly with the field. This is branch I. On this branch the magnetization $m(t) \approx -m_0$. As the field is increased to a positive value near the coercive field, there is a small time regime when the magnetization switches from $-m_0$ to a value near $+m_0$ (branch II). For larger fields, the magnetization has a roughly constant value near $+m_0$ (branch III). On decreasing the field to a small negative value, the magnetization retraces branch III for a while, then there is a quick switching of the magnetization from $+m_0$ to a value near $-m_0$ (branch IV). After this, there is again slow variation of the magnetization as the field changes (branch I), and the cycle repeats itself. As $\omega \to 0$, the loops contract, and the area of the hysteresis loop tends to decrease.

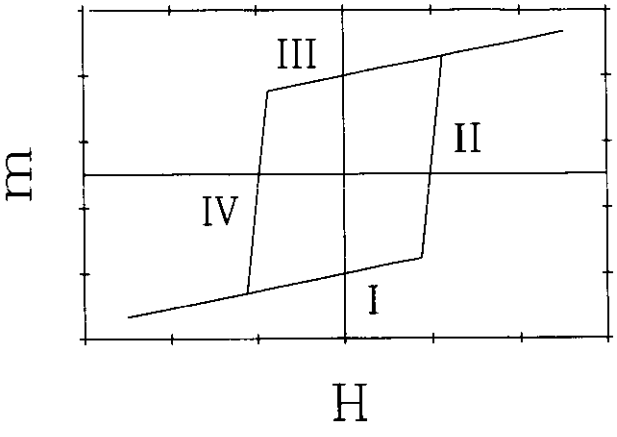

Figure 9. The hysteresis loop at low frequencies can be approximated as a parallelopiped. Lines I and III are approximately horizontal, and II and IV have large slopes.

Consider first the branch I. On this branch we have

$$m(t) \approx -m_0 . \tag{19}$$

We rewrite (14) as

$$A(t) = -\frac{H(t)}{m(t)} + \frac{2}{m(t)} \left(\frac{\mathrm{d}m}{\mathrm{d}H}\right) \left(\frac{\mathrm{d}H}{\mathrm{d}t}\right) . \tag{20}$$

Since on this branch the slope $\mathrm{d}m/\mathrm{d}H$ is small, and $\mathrm{d}H/\mathrm{d}t$ tends to zero as $H_0\omega$ when $\omega \to 0$, this implies that, to the leading-order terms in H_0 and ω, we may write

$$A(t) \simeq +\frac{H(t)}{m_0} + \text{terms of order } (H_0\omega) . \tag{21}$$

In figure 10 we show a graph of $A(t)$ versus ωt. Superposed on this is a graph of $-H(t)/m(t)$. We note that the two curves almost coincide except in the neighbourhood of t_c (by definition $m(t_c) = 0$), where the latter curve has a spurious singularity.

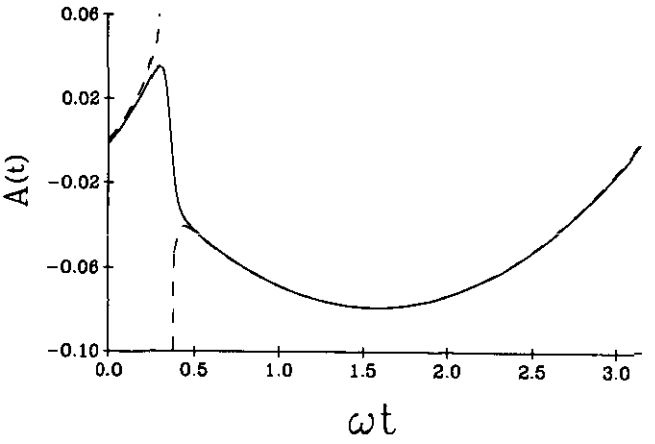

Figure 10. The behaviour of $A(t)$ as a function of ωt (full curve). The broken curve is its approximate expression $-H(t)/m(t)$, which is valid everywhere except near $t = t_c$, where this approximation has a spurious singularity.

For a given time dependence of $A(t)$, the evolution equation for $\tilde{C}_q(t)$ can be integrated as

$$\tilde{C}_q(t) = \tilde{C}_q(t_0) \exp\left(-q^2(t-t_0) + \int_{t_0}^{t} A(t')\,dt'\right) + T\int_{t_0}^{t} \exp\left(-q^2(t-t') + \int_{t'}^{t} A(t'')\,dt''\right) dt' . \tag{22}$$

Substituting for $A(t)$ the approximate value from (21), and letting t_0 tend to $-\infty$, we get

$$\tilde{C}_q(t) = T\int_{-\infty}^{t} \exp\left(-q^2(t-t') + \frac{1}{m_0}\int_{t'}^{t} H(t'')\,dt''\right) dt' . \tag{23}$$

When ω is very small, we note that $|H(t)| \ll H_0$ in the region of the loop where there are significant changes in $m(t)$ (branches II and IV in figure 9). Therefore for fields $H(t)$ less than the coercive field $H(t_c)$, $H(t)$ varies roughly linearly with time, and choosing the zero of the time coordinate to be when $H(t)$ crosses zero, we can write

$$H(t) = H_0\omega\, t + \text{higher order terms} . \tag{24}$$

Since the dependence of $H(t)$ when the magnetization changes significantly depends only on the product $(H_0\omega)$, it follows that in this limit, the dependence of the area W on H_0 and ω is of the form

$$W(H_0, \omega) = W(H_0\omega) . \tag{25}$$

In figure 11 we show three hysteresis curves for different values of H_0 and ω, keeping $(H_0\omega)$ unchanged. We see that the scaling equation (25) is obeyed to a very good approximation, even for these rather large values of ω, when the coercive field is close to H_0.

Using (24) in (23), we note that the integral over t' is a Gaussian integral, giving rise to an error function

$$\tilde{C}_q(t) \simeq T\sqrt{\frac{m_0\pi}{2H_0\omega}}\,\text{erfc}(z)\exp(z^2) \tag{26}$$

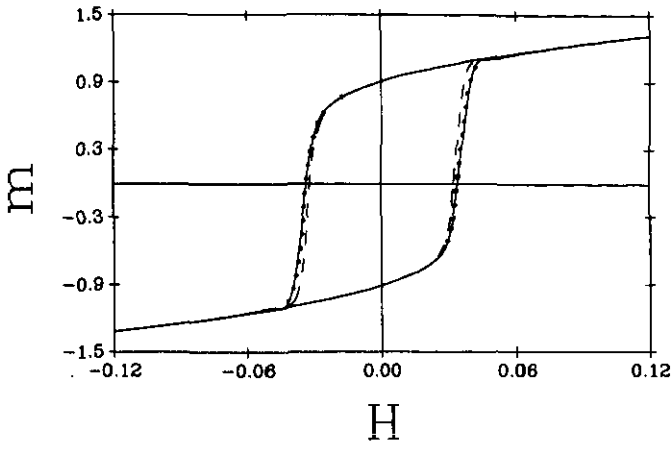

Figure 11. Graph of a superposition of three hysteresis loops with the same $H_0\omega$ product ($= 10^{-4}$). The loops are for $H_0 = 0.25$ (full curve), $H_0 = 0.1$ (dotted curve) and $H_0 = 0.05$ (broken curve).

where

$$z = \sqrt{\frac{m_0}{2H_0\omega}}\left(q^2 - \frac{H_0\omega t}{m_0}\right) \tag{27}$$

and

$$\operatorname{erfc}(z) = \frac{2}{\sqrt{\pi}}\int_z^\infty \exp\left(-x^2\right) \mathrm{d}x\,.$$

The error function $\operatorname{erfc}(z)$ varies asymptotically as $\exp\left(-z^2\right)/z\sqrt{\pi}$ for large z, and hence when $[q^2 - H(t)/m_0]$ is positive and large

$$\tilde{C}_q(t) \simeq \frac{T}{q^2 - H(t)/m_0}\,. \tag{28}$$

This is the value $\tilde{C}_q(t)$ would have if the system were in instantaneous thermal equilibrium at that value of the magnetic field. For small q, (28) is a good approximation to (26) only if $H(t)$ is negative, or small. For large positive $H(t)$ and small q, we cannot assume that the modes are in instantaneous thermal equilibrium. The equilibrium value of $\tilde{C}_{q\to 0}(H = 0)$ is infinite, but from (26), $\tilde{C}_q(t)$ can only grow at most to a value of order $T\sqrt{m_0/H_0\omega}$ for $q \to 0$ at $t = 0$. We have shown from (28) that for large q, $\tilde{C}_q(t)$ is approximately equal to T/q^2. The cross-over value q^* separating these small- and large-q regimes is thus given by

$$q^* = \left(\frac{H_0\omega}{m_0}\right)^{1/4}\,. \tag{29}$$

In figure 3, we compare the approximate solution (26) with the numerically determined solutions of $\tilde{C}_q(t)$ as a function of q at three different times $t_1 < 0$, $t_2 \sim 0$ and $t_3 = t_c$. In figure 4, we have plotted the numerically determined solution of $\tilde{C}_q(t)$ as a function of ωt as the field is swept from negative to positive values, at $q = 0$, $q = q^*$ and $q = 3q^*$, and also the theoretical approximation (26). Clearly, the approximation (26) is in agreement with the numerically determined $\tilde{C}_q(t)$ for all

times $t \lesssim t_c$ such that $|H(t)| \ll H_0$, and for all values of q. The approximation is not expected to work very well for large $|H(t)|$, as then $|m(t)|$ is significantly different from m_0. This causes a discrepancy of a few per cent between the precise values of $\tilde{C}_q(t)$ and the theoretical approximation. However, as is easily seen from these figures, the relative variations are very well captured in (26) even as $\tilde{C}_0(t)$ varies by more than three orders of magnitude. Modes with $q > q^*$ may be approximately described as being in instantaneous thermal equilibrium at all times, as is evident from the $q = 3q^*$ graph in figure 4.

When $q < q^*$, as t is increased to small positive values, $\tilde{C}_q(t)$ grows as $\exp(H_0\omega t^2/2m_0)$, and we get from (26)

$$\tilde{C}_q(t) \sim \frac{T}{\sqrt{H_0\omega}} \exp(H_0\omega t^2/2m_0 - q^2 t) .$$

This is a Gaussian distribution in q, with maximum at $q = 0$, whose width decreases as t increases. For $t \gg 1$, its width varies as $1/\sqrt{t}$. Hence integrating over all the q modes, we see that on branch I, the behaviour of $\tilde{S}(t)$ for positive $t \gg 1$ is given by

$$\tilde{S}(t) \simeq (\text{max height}) \times (\text{width})^d \simeq \frac{T}{\sqrt{H_0\omega}} t^{-d/2} \exp[H_0\omega t^2/2m_0] . \tag{30}$$

The approximation (19) breaks down if $\tilde{S}(t)$ becomes very large, as then $|m(t)|$ has to decrease to preserve the equality in (15). We thus conclude that the coercive time t_c is approximately given by the condition that $S(t_c)$ is of order r/u. The coercive field $H(t_c) \approx H_0\omega\, t_c$ is thus given by

$$H(t_c)^2 \sim H_0\omega \left| \ln \left[K\, T (H_0\omega)^{(d-2)/4} \right] \right|$$

where K is a constant. Since the contribution to the area W of the loops comes from its nearly rectangular section, $W \propto H(t_c)m_0$, yielding at low frequencies

$$W \sim \left\{ H_0\omega \left| \ln \left[K\, T (H_0\omega)^{(d-2)/4} \right] \right| \right\}^{1/2} . \tag{31}$$

Therefore in this limit, we find that the area of the loops obey the scaling form $W \sim H_0^{1/2}\,\omega^{1/2}$, with a logarithmic correction.

In figure 12 we show a log–log plot of the numerically determined solution of W/H_0 versus ω/H_0. There is also a low-frequency functional fit to the this curve from (31), which agrees well with the numerical data. We note that in the log–log plot, the graph below the critical frequency appears to the eye to be linear. The numerically determined slope of the curve between $\omega \sim 0.2$ and $\omega \sim 0.02$ is ≈ 0.34, so in this region, the area scales as $H_0^{0.66}\,\omega^{0.34}$, which is in agreement with the exponents obtained by RKP. However, at lower frequencies ($\omega \sim 0.001$), the slope increases to about 0.42, closer to its asymptotic value of $\frac{1}{2}$.

Using (31) we can find the relation between the critical field $H_c(\omega)$ when ω is small. In this case, as noted earlier, the loops are squarish, with the area of the loop $\approx 4m_0H_0$. This gives

$$H_c(\omega) = b\,\omega\, l |\ln [c/\omega]| \qquad \text{for small } \omega \tag{32}$$

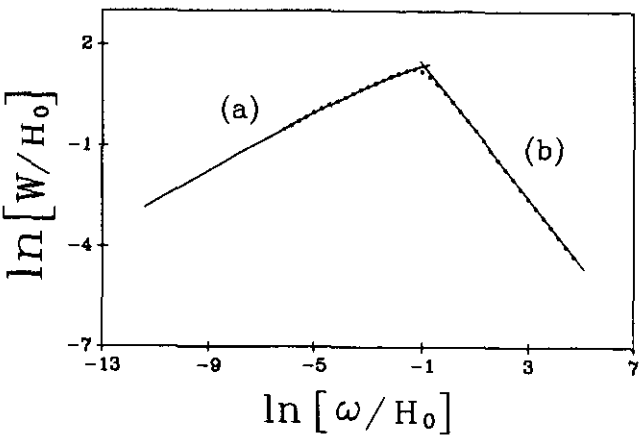

Figure 12. The log–log plot of W/H_0 versus ω/H_0 (circles) for $H_0 = 0.1$. The full curve (a) is the functional fit calculating the area from $W = a\sqrt{(H_0\omega)}\ln(K/H_0\omega)$, with $a = 4.94$ and $K = 0.0207$. The full curve (b) is the asymptotic high-frequency curve $W = \pi H_0^2/2\omega$.

where b and c are constants. We expect (32) to be the asymptotic form of the critical curve at low frequencies and fields.

We now determine the high-frequency behaviour of the system. At very high frequencies, the system does not have time to respond to the changing magnetic field. It is possible to make a $1/\omega$ expansion in the solution of (14) and (15) as follows. To lowest order, $m(t) = 0$ because the inversion symmetry of the loop is not broken (figure 6), and the solution is

$$m(t) \simeq 0 \qquad m_\perp^2(t) \simeq m_0^2 \qquad \tilde{C}_q(t) \simeq \frac{T}{q^2} \qquad A(t) \simeq 0\,.$$

Using these for the zeroth-order solution of the dynamical equations (14) and (15), we find to first order in $1/\omega$

$$m(t) = -\frac{H_0}{2\omega}\cos\omega t + \mathrm{O}(1/\omega^2)$$

and $m_\perp^2$, $\tilde{C}_q$ and A do not change. Using the fact that $\oint A(t)\,\mathrm{d}t = 0$, we find to next order in $1/\omega$

$$\begin{aligned} m(t) &= -\frac{H_0}{2\omega}\cos\omega t + \mathrm{O}(1/\omega^3) \qquad m_\perp^2(t) = m_0^2 - H_0^2/8\omega^2 + \mathrm{O}(1/\omega^3) \\ \tilde{C}_q(t) &= \frac{T}{q^2} + \mathrm{O}(1/\omega^3) \qquad A(t) = -\frac{u\,H_0^2}{8\omega^2}\cos\omega t + \mathrm{O}(1/\omega^3) \end{aligned} \tag{33}$$

and therefore the limiting form of the area of the loop is

$$W \simeq \frac{\pi H_0^2}{2\omega}\,. \tag{34}$$

In figure 6, which shows the typical high-frequency behaviour, it is clear that the m–H loop is almost perfectly elliptical, its maximum value being $H_0/2\omega$ as derived above. From figure 6, it is also clear that $m_\perp^2$ and $\tilde{S}(t)$ are both almost constant near the values derived here. From figure 12 we see that the high-frequency behaviour of the area agrees well with the solution given in (34).

In order to determine the critical curve, we set $m_\perp^2 = 0$ in (33), yielding to leading order

$$H_c(\omega) \simeq 2\sqrt{2}\, m_0\, \omega\,. \tag{35}$$

This asymptotic solution is superposed on the critical curve in figure 7. The agreement is very good when $H_0 \gtrsim 0.15$.

6. Summary and discussion

In this paper we have studied the dynamics of the O(N) symmetric model in the large-N limit, when it is subjected to a time-dependent magnetic field. We have shown the existence of a dynamical phase transition in this model signifying the onset of long-range order in the system with a non-zero average magnetization in a direction perpendicular to the applied field, and have determined the critical curve. At low frequencies, the area follows the approximate scaling law $W \sim (H_0\omega)^{1/2}$, with logarithmic corrections. There is also scaling at high frequencies where the area scales as H_0^2/ω. We have found that these results are true for all $d > 2$.

These power laws are robust, in the sense that no fine tuning of temperature is necessary. The system shows this power-law behaviour, so long as the temperature is not too close to the critical temperature. They occur in a dissipative system with nonlinear dyanamics. Hysteresis thus provides one of the simplest-to-understand examples of self-organized criticality [11], a concept that has received much attention lately.

Of course, these power laws are seen only for values of H_0 near zero. We note that $H_0 = 0$ is a line of first-order phase transitions in the H_0–T plane. We have noted earlier [12] that systems on the first-order phase boundary, more precisely in the two-phase coexistence region, show self-organized critical behaviour. In equilibrium statistical mechanics the two-phase coexistence region is special, as changes in the order parameter do not give rise to corresponding changes in the conjugate field. This implies that fluctuations can grow to large values as the thermodynamical restoring force is zero. In non-equilibrium systems, this gives rise to very slow changes (power-law growth or decay in time) in properties, for example in phase separation. To the extent that the magnetization $m(t)$ lies between $-m_0$ and $+m_0$ in the time when hysteresis effects are significant, one is justified in saying that we see power laws in hysteresis because in this process, the system is driven so that it lies in the two-phase coexistence region.

We note that our analysis is equivalent to a spin-wave approximation of the magnetization dynamics (the large-N limit makes the spin waves for different modes effectively decouple). In this case, the gapless nature of the spin-wave excitation spectrum at $H = 0$ is crucial to get the spin-wave instability, which allows the magnetization direction to turn continuously. The importance of Goldstone modes in self-organized criticality has been noted earlier [12, 13]. For magnetic systems, the power-law tails in magnetic relaxation in the context of self-organized criticality have been discussed by Nowak and Usadel [14], and also by Newman *et al* [15].

We have shown that there is a length scale $L^*(H_0,\omega) \sim (H_0\omega)^{-1/4}$ corresponding to the inverse of q^* in (29), which can be interpreted as a dynamical correlation length. At zero frequency $L^* \to \infty$, which is consistent with the power-law tail in

the transverse correlation function when $H = 0$. These results continue to hold for finite-N systems within the spin-wave approximation. Using dynamical renormalization arguments we have found that the low-frequency result $\alpha = \beta = \frac{1}{2}$ remains unchanged even for finite N. Hence the 'universality class' of the low-frequency scaling behaviour of the area of the hysteresis loop includes all isotropic $N \geqslant 2$ vector models with short-ranged ferromagnetic interactions, in all dimensions $d > 2$. The details of this analysis will be given in a forthcoming publication.

Of course, the model studied is highly simplified, and effects of magnetic anisotropy, dipolar forces, magneto-elastic couplings and eddy currents have not been included. Inclusion of these effects can substantially alter the qualitative behaviour of hysteresis loops. For example, in the presence of magnetic anisotropy the spins do encounter a free-energy barrier, and our analysis does not apply. Dipolar forces give rise to domain formation in zero external field, and a large component of the response to small external fields then comes from the motion of domain walls. All such effects have been excluded from our analysis. The model we studied can at best describe hysteresis in small particles of magnetic materials with small anisotropy, embedded in an insulating matrix (the size of the individual particles should be $\lesssim 10\ \mu$m so that each contains only a single magnetic domain). A theoretical description of hysteresis incorporating these effects remains a challenge.

Acknowledgments

We thank H R Krishnamurthy and R Pandit for a critical reading of an earlier version of this manuscript, M Acharyya, B K Chakrabarti, M Mahato and S R Shenoy for communicating their results prior to publication, and V Krishnamurthy for help with the figures.

References

[1] Agarwal G S and Shenoy S R 1981 *Phys. Rev.* A **23** 2719
Shenoy S R and Agarwal G S 1984 *Phys. Rev.* A **29** 1315
[2] Mahato M and Shenoy S R 1992 *Preprint Hyderabad University*
[3] Tomé T and de Oliveira M J 1990 *Phys. Rev.* A **41** 4251
[4] Jung P, Gray G and Roy R 1990 *Phys. Rev. Lett.* **65** 1873
[5] Rao M, Krishnamurthy H R and Pandit R 1990 *Phys. Rev.* B **42** 856; 1991 *J. Phys.: Condens. Matter* **1** 9061
[6] Acharyya M and Chakrabarti B K 1992 unpublished
[7] Lo W S and Pelcovits R A 1990 *Phys. Rev.* A **42** 7471
[8] Sengupta S, Marathe Y J and Puri S 1992 *Phys. Rev.* B **45** 7828
[9] Mazenko G and Zannetti M 1985 *Phys. Rev.* B **32** 4565
[10] Press W H, Flannery B P, Teukolsky S A and Vetterling W T 1989 *Numerical Recipes* (Cambridge: Cambridge University Press)
[11] Bak P, Tang C and Weisenfeld K 1987 *Phys. Rev. Lett.* **59** 381; 1988 *Phys. Rev.* A **38** 364
[12] Dhar D and Majumdar S N 1990 *J. Phys. A: Math. Gen.* **23** 4333
[13] Obhukov S P 1990 *Phys. Rev. Lett.* **65** 1395
[14] Nowak U and Usadel K D 1990 *Physica* **165B** 211; 1991 *Phys. Rev.* B **43** 851
[15] Newman T J, Bray A J and Moore M A 1990 *Phys. Rev.* B **42** 4514